The influence of a human hand-arm system on the vibrational dynamic behaviour of a compliant mechanical structure

Sébastien S Perrier, Yvan Champoux and Jean-Marc Drouet

Abstract
The aim of this study is to provide an approach to predicting human influence on a compliant mechanical structure using a substructuring technique. Substructuring techniques allow us to obtain detailed information on the vibrational behaviour of an assembly of structures by characterization of each structure separately. In this manuscript, a hand-arm system is coupled with a vibrating structure using a substructuring technique. A lightweight and compliant vibrating beam is used to demonstrate the concept. To demonstrate the feasibility of accurately predicting the hand-arm systems' influence on the beam, we selected one position and tested it using four push forces. The characteristics of the hand-arm system for each configuration were coupled with the dynamic characteristics of the beam only over a frequency range of [5; 300] Hz. For each of the four configurations, the coupling predicts the influence of the hand on the vibrational behaviour of the beam. Reliable predictions were obtained for the vibrational behaviour of the assembly. The results indicate that the substructuring approach predicted the vibrational behaviour of the hand-arm-beam assembly with less than 3% error.

1. Introduction

Many people, due to various work and recreational activities, are exposed to vibration through physical contact with a vibrating structure. Exposure to vibration can be perceived as a source of discomfort, or may sometimes result in a complex combination of vascular, neurological and musculoskeletal disorders (Griffin, 1990; Mansfield, 2005). The study of interactions between humans and structures is thus essential to reducing transmitted vibration. Included in these interactions, hand-transmitted vibration has always been a major concern. Hence, the study of hand-arm systems with vibration is important to understanding mechanisms of vibration transmission phenomena, assessing vibration exposure and developing better tools and vibration-reducing devices (Reynolds and Soedel, 1977; Burström, 1990; Griffin, 1994; Dong et al., 2001).

When the hand-arm system is coupled to a vibrating mechanical structure, the resulting vibrational behaviour of the coupled hand-structure system is complex. As part of the understanding on vibration transmission phenomena, the biodynamic response of the entire hand-arm system has been investigated in several studies (Gurram et al., 1995; Burström, 1997; Aldien et al., 2005; Dong et al., 2005). The International Standard ISO-5349 (ISO-5349) (2001) specifies methods for measuring, evaluating, and reporting exposures to hand-transmitted vibration. Among the biodynamic responses, the driving-point mechanical impedance has been extensively studied in order to improve our understanding of the biodynamic response of the hand-arm system to vibration excitations in three orthogonal axes (Jahn and Hesse, 1986; ISO-10068, 2012, Dong et al., 2012). Previous studies have provided valuable insight into the coupling effects between the human hand-arm system and vibrating structures such as tools. For example, the use of the human

VélUS Research Group, Group of Acoustics and Vibration, Department of Mechanical Engineering, Sherbrooke University, QC, Canada

Corresponding author:
Sébastien Perrier, Department of Mechanical Engineering, Université de Sherbrooke, 2500 boul. de l'Université, Sherbrooke (QC) J1K 2R1, Canada.
Email: sebastien.perrier@usherbrooke.ca

vibration models developed over the past 40 years for the analyses or designs of the tools actually consider the coupling effects (Mishoe and Suggs, 1977; Reynolds and Falkenberg, 1982, 1984; Daikoku and Ishikawa, 1990; Gurram et al., 1995; Rakheja et al., 2002; ISO-10068, 2012). In some cases, the hand-arm system actually has little effect on the tool vibration because the apparent mass is small compared to the tool mass (Marcotte et al., 2010; Dong et al., 2008b). However, where the hand-arm system has a significant influence on the dynamic behaviour of the human – structure assembly, none of these studies enable us to know the influence of the hand-arm system on the dynamic behaviour in compliant mechanical structures.

Meanwhile, knowledge of interactions between structure assemblies was a major concern in mechanical engineering. Since the 1960s, substructuring techniques have emerged as a focus of research in structural dynamics. These substructuring techniques can be used on mechanical structures to study and improve the dynamic behavior of complex assemblies by analyzing the behavior of each substructure separately. A rapid overview of these techniques is provided below to establish the context for the approach used in this study:

- Dynamic substructuring ideas as reduction techniques (Hurty, 1960).
- 1960s–1970s: "Component-Mode Synthesis" methods (CMS) with some major developments resulting in classic methods (Craig and Bampton, 1968; MacNeal, 1971; Rubin, 1975).
- 1980s: Substructuring coupling techniques became attractive to the experimental community. These techniques dealt with structural dynamic modification (SDM) with the aim to alter the dynamic behaviour of a base structure by coupling a "modification" structure (usually lumped masses or springs).
- 1980s–1990s: Coupling techniques were directly applied to measured frequency response functions (FRFs). This resulted in the "Impedance coupling" technique (Imregun and Robb, 1992) and the "FBS: Frequency-Based Substructuring" technique (Jetmundsen, 1986; Jetmundsen et al., 1988).

Detailed review articles on coupled/modified structures techniques can be found in the literature (Ewins, 2000; Avitabile, 2003; De Klerk et al., 2008).

Although substructuring techniques exist for several years, to authors' knowledge, no one has used these techniques when one of the substructures is the human body. In the context of vibration transmitted to the human body, the coupling techniques using FRFs developed during the 1980s and 1990s can be useful to study human – structure assemblies in order to reduce transmitted vibration.
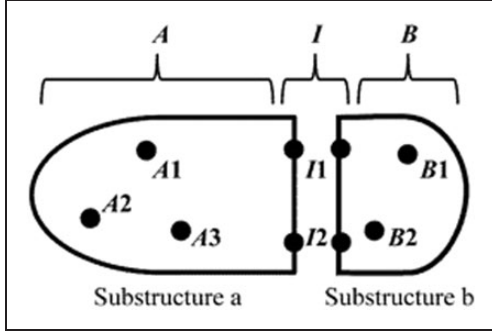
Based on this verification, the primary objective of this paper is to provide an approach to studying human influence on compliant mechanical structures. Our approach combines a biodynamic characterization of the human body with the vibrational behaviour of a mechanical structure to predict the vibrational behaviour of the assembly. This approach uses substructuring techniques with biodynamic characterizations and dynamic characterizations of the mechanical structure separately to describe and predict the vibrational behaviour of a human-structure assembly.

To demonstrate, this study focuses on the mechanical coupling performed between the hand-arm system and a straight lightweight beam. This paper presents the mathematical developments for the coupling approach, the method to determine the biodynamic response of the hand-arm system as well as the method to characterize the vibrational behaviour of the beam alone. The biodynamic response of the hand-arm system depends on several parameters such as posture, type of excitation, grip and push forces, and others (Gurram et al., 1995; Burström, 1997; Aldien et al., 2005, 2006; Besa et al., 2007). The approach to predicting the influence of the hand-arm system on the beam's dynamic behaviour was thus used while controlling various parameters. One specific posture of the hand-arm system has been chosen and four different push forces were tested. In this paper, the biodynamic responses of the hand-arm system in terms of mechanical impedances are revealed for the specific posture and the four push forces used. Moreover, a comparison is made between the vibrational behaviours of the assembly obtained using direct experimental measurements and the predictions from the substructuring approach.
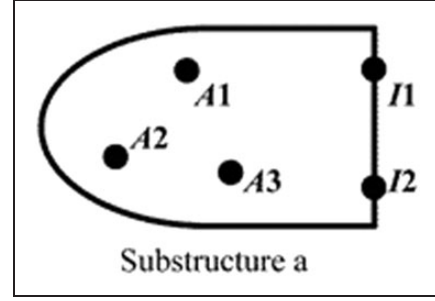
2. Methods

In the first section, the approach and formulation of the coupling technique between two substructures is presented in a general way in terms of impedance. The second section focuses specifically on the substructuring approach with biodynamics in terms of impedance. In the third section, equations to couple the hand-arm system with the beam are formulated. The formulation in terms of FBS, or mobility, is disclosed in the Appendix 1. These formulations enable us to obtain the vibrational behaviour of the assembly or coupling system by taking into account the vibrational behaviour of each substructure separately. The methodology choice between a FBS formulation and an impedance formulation depends mainly on the kind of configuration that has to be tested and is up to the users.

The method used to conduct the experimental measurements directly on the assembly is presented in the fourth section. The experimental data are used to evaluate the accuracy of the substructuring approach in

Figure 1. Example of a coupling between two substructures "a" and "b" where substructure "a" has five points of interest (two of them are in the interface set *I* and three are in the internal set *A*) and substructure "b" has four points of interest (two of them are in the interface set *I* to match those of substructure "a" and two are in the internal set *B*).

predicting the assembly's vibrational behaviour. The method to characterize the structures vibrational behaviour is presented in the fifth section for the beam and in the final section for the hand-arm system.

2.1. Approach and formulation of the coupling technique

This section introduces the terminology and notations for a coupled system with two substructures. Equations are developed to present the dynamic behaviour of the coupled system by characterization of each structure separately. As an illustrative example, two substructures "a" and "b" are coupled to form an assembly "ab" (Figure 1). In the following equations, these structures are described with superscript lowercase letters. The subscript capital letters *A*, *B* and *I* represent respectively the set of internal degrees of freedom (DOFs) for substructure "a", the set of internal DOFs for substructure "b", and the set of interface DOFs between substructures "a" and "b". Finally, upright bold formatting is used to represent matrices or vectors.

These two substructures can be described independently by an impedance formulation. In an impedance characterization, all the points of interest are blocked.

Figure 2. Illustration of each point involved in the characterization for substructure "a".

The only point that is freed is the point where the excitation takes place. The points of interest are the interface points with other structures, the points where the boundary conditions are applied and any other points that need to be considered. Let consider substructure "a" alone as shown in Figure 2. One can write the following equation for substructure "a"

$$\begin{Bmatrix} \mathbf{F}_A^a(\omega) \\ \mathbf{F}_I^a(\omega) \end{Bmatrix} = \begin{bmatrix} \mathbf{Z}_{AA}^a(\omega) & \mathbf{Z}_{AI}^a(\omega) \\ \mathbf{Z}_{IA}^a(\omega) & \mathbf{Z}_{II}^a(\omega) \end{bmatrix} \begin{Bmatrix} \mathbf{V}_A^a(\omega) \\ \mathbf{V}_I^a(\omega) \end{Bmatrix} \quad (1)$$

where $\mathbf{Z}_{AI}^a(\omega)$ is an impedance characterization for substructure "a". The first subscript letter *A* represents the location in terms of resulting blocked force and the second subscript letter *I* represents the velocity excitation location.

For the sake of simplicity in the following equations, the frequency-dependency (ω) of the various terms is not written. Equation (1) can be detailed for substructure "a" in the following manner.

$$\begin{Bmatrix} \mathbf{F}_{A1}^a \\ \mathbf{F}_{A2}^a \\ \mathbf{F}_{A3}^a \\ \mathbf{F}_{I1}^a \\ \mathbf{F}_{I2}^a \end{Bmatrix} = \begin{bmatrix} \mathbf{Z}_{A1A1}^a & \mathbf{Z}_{A1A2}^a & \mathbf{Z}_{A1A3}^a & \mathbf{Z}_{A1I1}^a & \mathbf{Z}_{A1I2}^a \\ \mathbf{Z}_{A2A1}^a & \mathbf{Z}_{A2A2}^a & \mathbf{Z}_{A2A3}^a & \mathbf{Z}_{A2I1}^a & \mathbf{Z}_{A2I2}^a \\ \mathbf{Z}_{A3A1}^a & \mathbf{Z}_{A3A2}^a & \mathbf{Z}_{A3A3}^a & \mathbf{Z}_{A3I1}^a & \mathbf{Z}_{A3I2}^a \\ \mathbf{Z}_{I1A1}^a & \mathbf{Z}_{I1A2}^a & \mathbf{Z}_{I1A3}^a & \mathbf{Z}_{I1I1}^a & \mathbf{Z}_{I1I2}^a \\ \mathbf{Z}_{I2A1}^a & \mathbf{Z}_{I2A2}^a & \mathbf{Z}_{I2A3}^a & \mathbf{Z}_{I2I1}^a & \mathbf{Z}_{I2I2}^a \end{bmatrix} \begin{Bmatrix} \mathbf{V}_{A1}^a \\ \mathbf{V}_{A2}^a \\ \mathbf{V}_{A3}^a \\ \mathbf{V}_{I1}^a \\ \mathbf{V}_{I2}^a \end{Bmatrix} \quad (2)$$

$$\mathbf{Z}_{A1A1}^a = \begin{bmatrix} Z_{A1xA1x}^a & Z_{A1xA1y}^a & Z_{A1xA1z}^a & Z_{A1xA1\theta x}^a & Z_{A1xA1\theta y}^a & Z_{A1xA1\theta z}^a \\ Z_{A1yA1x}^a & Z_{A1yA1y}^a & Z_{A1yA1z}^a & Z_{A1yA1\theta x}^a & Z_{A1yA1\theta y}^a & Z_{A1yA1\theta z}^a \\ Z_{A1zA1x}^a & Z_{A1zA1y}^a & Z_{A1zA1z}^a & Z_{A1zA1\theta x}^a & Z_{A1zA1\theta y}^a & Z_{A1zA1\theta z}^a \\ Z_{A1\theta xA1x}^a & Z_{A1\theta xA1y}^a & Z_{A1\theta xA1z}^a & Z_{A1\theta xA1\theta x}^a & Z_{A1\theta xA1\theta y}^a & Z_{A1\theta xA1\theta z}^a \\ Z_{A1\theta yA1x}^a & Z_{A1\theta yA1y}^a & Z_{A1\theta yA1z}^a & Z_{A1\theta yA1\theta x}^a & Z_{A1\theta yA1\theta y}^a & Z_{A1\theta yA1\theta z}^a \\ Z_{A1\theta zA1x}^a & Z_{A1\theta zA1y}^a & Z_{A1\theta zA1z}^a & Z_{A1\theta zA1\theta x}^a & Z_{A1\theta zA1\theta y}^a & Z_{A1\theta zA1\theta z}^a \end{bmatrix} \quad (3)$$

In a general way, this equation includes all the DOFs for points $A1$, $A2$, $A3$, $I1$ and $I2$. For example, the matrix $\mathbf{Z}^{\mathrm{a}}_{A1A1}$ from equation (2) can be detailed with all these DOFs.

In general, sets A, B and I are used in the following equations to characterize substructures "a" and "b". Substructure "b" can also be described by an impedance formulation

$$\left\{ \begin{array}{c} \mathbf{F}^{\mathrm{b}}_I \\ \mathbf{F}^{\mathrm{b}}_B \end{array} \right\} = \left[\begin{array}{cc} \mathbf{Z}^{\mathrm{b}}_{II} & \mathbf{Z}^{\mathrm{b}}_{IB} \\ \mathbf{Z}^{\mathrm{b}}_{BI} & \mathbf{Z}^{\mathrm{b}}_{BB} \end{array} \right] \left\{ \begin{array}{c} \mathbf{V}^{\mathrm{b}}_I \\ \mathbf{V}^{\mathrm{b}}_B \end{array} \right\} \qquad (4)$$

With regard to the complete system or assembly "ab": similar to substructure "a" in equation (1) and substructure "b" in equation (4), the impedance version of the FRF matrix for the complete system "ab" can be expressed as

$$\left\{ \begin{array}{c} \mathbf{F}^{\mathrm{ab}}_A \\ \mathbf{F}^{\mathrm{ab}}_I \\ \mathbf{F}^{\mathrm{ab}}_B \end{array} \right\} = \left[\begin{array}{ccc} \mathbf{Z}^{\mathrm{ab}}_{AA} & \mathbf{Z}^{\mathrm{ab}}_{AI} & 0 \\ \mathbf{Z}^{\mathrm{ab}}_{IA} & \mathbf{Z}^{\mathrm{ab}}_{II} & \mathbf{Z}^{\mathrm{ab}}_{IB} \\ 0 & \mathbf{Z}^{\mathrm{ab}}_{BI} & \mathbf{Z}^{\mathrm{ab}}_{BB} \end{array} \right] \left\{ \begin{array}{c} \mathbf{V}^{\mathrm{ab}}_A \\ \mathbf{V}^{\mathrm{ab}}_I \\ \mathbf{V}^{\mathrm{ab}}_B \end{array} \right\} \qquad (5)$$

The impedance formulation (equation (5)), corresponding to the dynamic behavior of the coupled system "ab", can be predicted based on the impedance characterization of each substructure separately (equations (1) and (4)). According to substructuring techniques, this is enabled using the equilibrium and compatibility conditions at the interface set of DOFs. An impedance version of the FRF matrix for the coupled structure "ab" is derived as

$$\left[\begin{array}{ccc} \mathbf{Z}^{\mathrm{ab}}_{AA} & \mathbf{Z}^{\mathrm{ab}}_{AI} & 0 \\ \mathbf{Z}^{\mathrm{ab}}_{IA} & \mathbf{Z}^{\mathrm{ab}}_{II} & \mathbf{Z}^{\mathrm{ab}}_{IB} \\ 0 & \mathbf{Z}^{\mathrm{ab}}_{BI} & \mathbf{Z}^{\mathrm{ab}}_{BB} \end{array} \right] = \left[\begin{array}{ccc} \mathbf{Z}^{\mathrm{a}}_{AA} & \mathbf{Z}^{\mathrm{a}}_{AI} & 0 \\ \mathbf{Z}^{\mathrm{a}}_{IA} & \mathbf{Z}^{\mathrm{a}}_{II} + \mathbf{Z}^{\mathrm{b}}_{II} & \mathbf{Z}^{\mathrm{b}}_{IB} \\ 0 & \mathbf{Z}^{\mathrm{b}}_{BI} & \mathbf{Z}^{\mathrm{b}}_{BB} \end{array} \right] \qquad (6)$$

2.2. Formulation of the substructuring approach with biodynamics

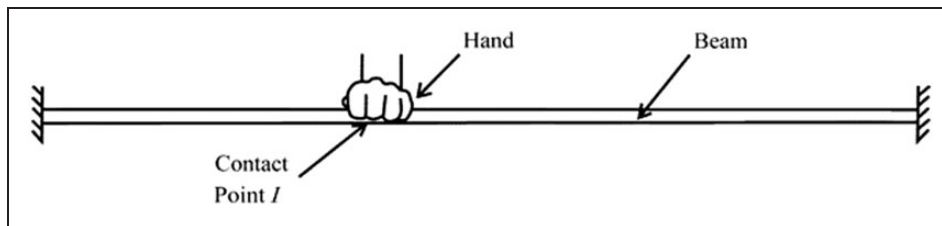In this article, the hand-arm system is coupled to a beam (Figure 3).

This example contextualizes the coupling technique between substructures. The "Impedance coupling" technique (Imregun and Robb, 1992) is formulated to present the substructuring approach coupling the hand-arm system with the beam. From now on, substructure "a" represents the mechanical structure, substructure "b" the hand-arm system and the interface I is the contact between the hand-arm system and the mechanical structure. As an approach to predicting the influence of the human, wherein the human is coupled to a vibrating structure, the substructuring techniques offer some advantages that can be used either with biodynamic measurements, representative models, or other characterizations of the human body. One of these advantages is the opportunity of coupling substructures through consideration of their interface set only. Since only interface measurements can be gathered for the human body, namely the driving-point, equation (6) can be simplified to eliminate the set of internal DOFs B

$$\left[\begin{array}{cc} \mathbf{Z}_{AA} & \mathbf{Z}_{AI} \\ \mathbf{Z}_{IA} & \mathbf{Z}_{II} \end{array} \right]^{\mathrm{ab}} = \left[\begin{array}{cc} \mathbf{Z}^{\mathrm{a}}_{AA} & \mathbf{Z}^{\mathrm{a}}_{AI} \\ \mathbf{Z}^{\mathrm{a}}_{IA} & \mathbf{Z}^{\mathrm{a}}_{II} + \mathbf{Z}^{\mathrm{b}}_{II} \end{array} \right] \qquad (7)$$

Equation (7) is the generalized equation of the substructuring approach with biodynamics in terms of impedance formulation. In this equation, each term is a matrix and there could be as many DOFs as necessary for the internal set of points A and the interface set of points I.

2.3. Equations coupling the hand-arm system with a beam

To implement and test the limits of the approach, a beam was chosen as the mechanical structure. This beam is a circular cylinder with a diameter of 25.4 mm, a wall thickness of 3.2 mm, and a total length of 168 cm. The beam was clamped at both ends on 2 rigid steel posts which were firmly attached to a heavy and rigid steel table. This structure was chosen to reveal multiple modes in the frequency

Figure 3. Configuration for the example of the hand-arm system coupled to a beam.

range of interest 5 – 300 Hz. The Figure 4 illustrates the configuration of the beam.

This configuration is different from the theoretical example presented in the previous section (Figure 2). In this configuration, internal set A contains two points, namely $A1$ and $A2$, and set I contains only one point. Using equations (5) and (7) for the coupling of the beam with the hand-arm system in this configuration, one can write

$$\begin{Bmatrix} \mathbf{F}_{A1}^{ab} \\ \mathbf{F}_{A2}^{ab} \\ \mathbf{F}_{I}^{ab} \end{Bmatrix} = \begin{bmatrix} \mathbf{Z}_{A1A1}^{a} & \mathbf{Z}_{A1A2}^{a} & \mathbf{Z}_{A1I}^{a} \\ \mathbf{Z}_{A2A1}^{a} & \mathbf{Z}_{A2A2}^{a} & \mathbf{Z}_{A2I}^{a} \\ \mathbf{Z}_{IA1}^{a} & \mathbf{Z}_{IA2}^{a} & \mathbf{Z}_{II}^{a} + \mathbf{Z}_{II}^{b} \end{bmatrix} \begin{Bmatrix} \mathbf{V}_{A1}^{ab} \\ \mathbf{V}_{A2}^{ab} \\ \mathbf{V}_{I}^{ab} \end{Bmatrix} \quad (8)$$

Since the beam is clamped in $A1$ and $A2$ ($\mathbf{V}_{A1}^{ab} = \mathbf{V}_{A2}^{ab} = 0$), equation (8) leads to

$$\begin{Bmatrix} \mathbf{F}_{A1}^{ab} \\ \mathbf{F}_{A2}^{ab} \\ \mathbf{F}_{I}^{ab} \end{Bmatrix} = \begin{bmatrix} \mathbf{Z}_{A1I}^{a} \\ \mathbf{Z}_{A2I}^{a} \\ \mathbf{Z}_{II}^{a} + \mathbf{Z}_{II}^{b} \end{bmatrix} \{\mathbf{V}_{I}^{ab}\} \quad (9)$$

Equation (9) can also be simplified to highlight the dynamic behaviour of the assembly in the coupling point I which is the point of interest when studying human-structure interactions.

$$\{\mathbf{F}_{I}^{ab}\} = [\mathbf{Z}_{II}^{a} + \mathbf{Z}_{II}^{b}]\{\mathbf{V}_{I}^{ab}\} \quad (10)$$

Among the available DOFs, only the vertical z-axis is considered in this application. The beam is excited in the vertical direction only. Equation (10) can be reduced in the following manner

$$\{F_{Iz}^{ab}\} = [Z_{IzIz}^{a} + Z_{IzIz}^{b}]\{V_{Iz}^{ab}\} \quad (11)$$

2.4. Experimental data on the coupled system for model validation

Experimental data were measured to evaluate the accuracy of the predictions of the influence of the human hand on the dynamic behaviour of the circular cylinder beam. Impedance of the coupled system (hand on beam) was measured using a force transducer and an accelerometer integrated in the frequency domain to obtain the velocity. These sensors were installed under the beam where the hand was located (Figure 5). A random vibration signal (white noise) was provided to the shaker within the frequency range of 5–300 Hz with an RMS value of $10\,\mathrm{m/s^2}$ over the frequency range of interest. The acquisition system was Test.Lab 11B software from LMS. The study was carried out using one subject to avoid inter-subject variability. One hand-arm posture was chosen for impedance measurements in the vertical direction (See subsection Experimental determination of the hand-arm system's biodynamic response). A total of 4 different push forces were
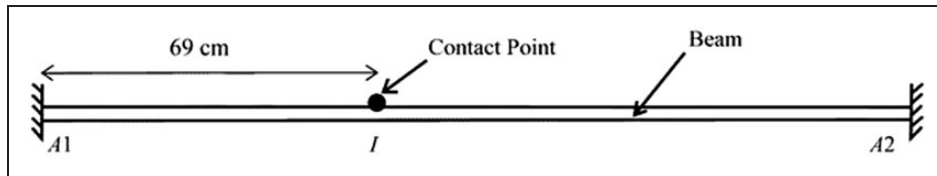

Figure 4. Configuration of the beam to be coupled with the hand-arm system.
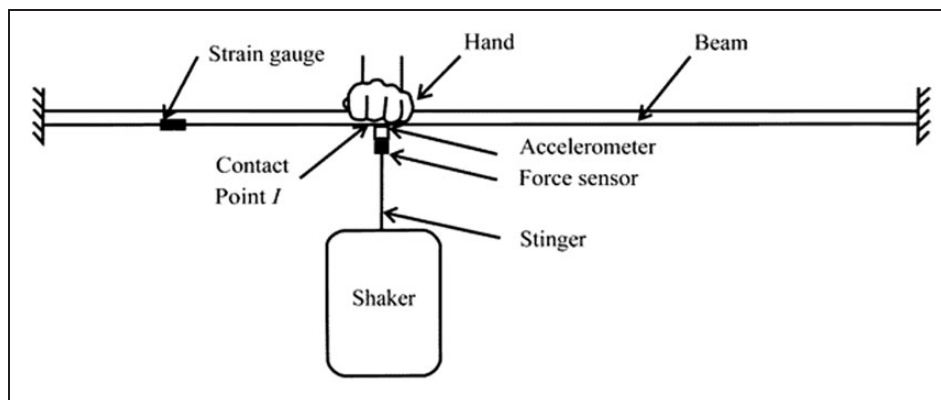

Figure 5. Experimental setup to measure the dynamic behaviour of the assembly (beam + hand) for 4 different push forces of the hand at contact point I (Force sensor 208C03 type ICP from PCB Piezotronics, Accelerometer 356B20 type ICP from PCB Piezotronics, Strain gauge with signal conditioner type P-3500 from Vishay for the strain gauge measurement).

tested at 20, 30, 40, and 50 N. The push force was measured and controlled using a strain gauge installed on the beam. For each configuration, the subject was requested to lean on the beam without applying any grip force and maintain a constant push force during the exposure by looking at the force level displayed on the strain gauge signal conditioner (Figure 5). After the correct posture and push force were established, the vibration data were measured.

2.5. Dynamic characterization of the beam

For the dynamic characterization of the beam alone, the FRF required in terms of impedance Z_{IzIz}^{a} for the coupling process (equation 11) was obtained experimentally using the same procedure described in Experimental data on the coupled system for model validation section without the hand on the beam. The frequency resolution for the harmonic response of the structure was 0.5 Hz.
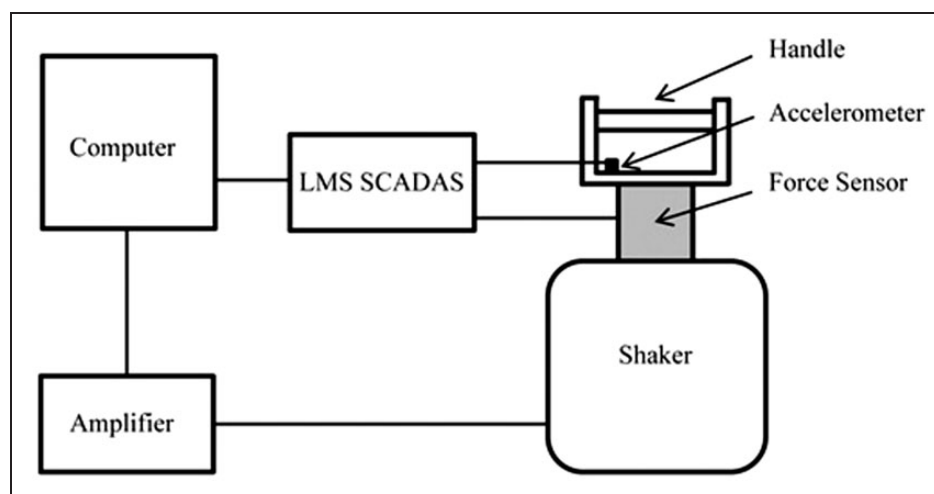
2.6. Experimental determination of the hand-arm system's biodynamic response

A few studies have investigated the effects of some of the influencing factors such as vibration direction, hand and arm posture, applied hand forces, vibration spectra, and others on the biodynamic response characteristics of the entire hand-arm system (Gurram et al., 1995; Burström, 1997; Aldien et al., 2005, 2006; Besa et al., 2007). Although the biodynamic response characteristics have been measured on human subjects under controlled test cond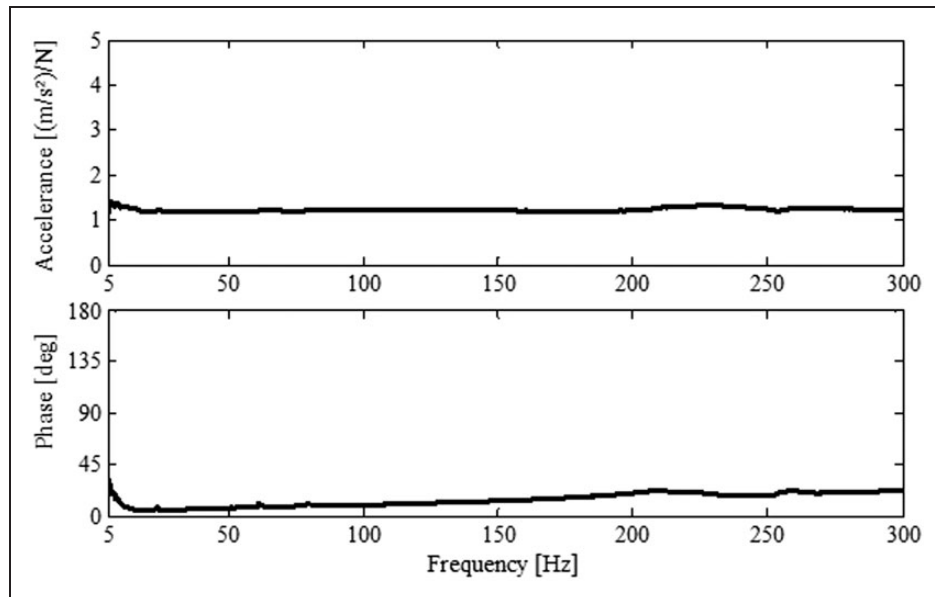itions, considerable differences are known to exist in the impedance data reported by different investigators (Gurram et al., 1995; ISO-10068, 2012; Rakheja et al., 2002; Adewusi et al., 2008). These differences may be attributable, in part, to the different methods and test conditions employed by individual investigators, and to the dependence of the biodynamic response characteristics on the influencing factors previously cited.

For these reasons, the hand-arm system is characterized in this study in terms of measured impedance using controlled conditions. Application of the substructuring method requires knowledge of reliable data on the hand-arm impedance corresponding to particular postures, hand forces and vibration levels. In equation (11), Z_{IzIz}^{b} corresponds to the driving-point mechanical impedance of the hand-arm system under a vertical z-axis excitation. This frequency dependent term was measured to get the experimental FRF of the hand-arm system's dynamic characteristics. Specifically, this was obtained using a specially designed handle with the same characteristics as the circular cylinder used for the beam. This handle was equipped with an accelerometer and mounted on a force sensor installed on a shaker allowing impedance measurements (Figure 6). The acquisition system was the same Test.Lab 11B software from LMS. To avoid any inherent nonlinear dynamic properties of the hand-arm system, the same acceleration signal was provided to the handle. This was done using the Vibration Research Corporation field data replication system. Measurements were performed within the frequency range of 5 – 300 Hz with a 0.5 Hz resolution.

The mass of the hand fixture – force sensor assembly is 1.4 kg. The response spectrum of the empty handle

Figure 6. Diagram of the hand-arm impedance measurement system (LMS Test.Lab 11b software with SCADAS mobile front-end, Power amplifier SS250VCF from MB Dynamics for the shaker, 6 DOFs force sensor model MC3-6-500 from AMTI, Accelerometer 356B20 type ICP from PCB Piezotronics).

Figure 7. Accelerance of the empty handle (without hand coupling).

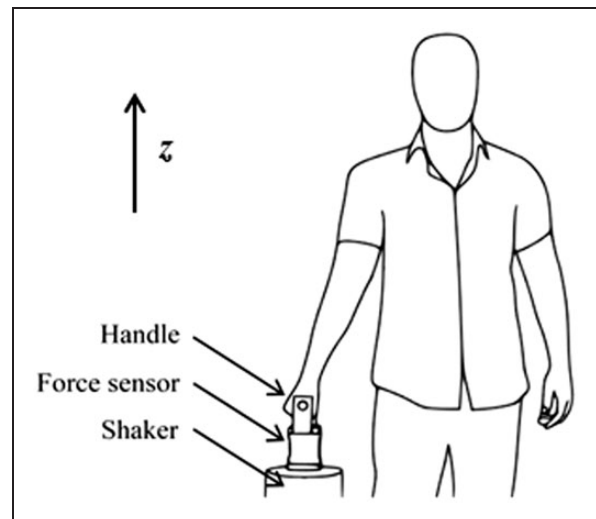(without hand coupling) is presented in Figure 7 because in terms of accelerance.

According to this spectrum (Figure 7), it can be seen that the fundamental resonant frequency of the empty handle with force sensor is well above 300 Hz.

Previous studies have investigated the effect of the handle dynamics on the biodynamic measurements (Marcotte et al., 2005, 2007; Dong et al., 2008a). Since the handle is considered rigid in the frequency range of interest (Figure 7), the handle impedance can be subtracted from the total impedance (hand + handle) to obtain the hand-arm system mechanical impedance (Dong et al., 2006; Besa et al., 2007). Measurements were done with and without a hand on the handle.

$$Z_{\text{Hand}} = Z_{\text{Total}} - Z_{\text{Handle}} \qquad (12)$$

Measurements were carried with the same subject to avoid inter-subject variability. The same hand-arm posture that was used for measurement on the beam was used for hand impedance measurements in the vertical direction. The angle between the upper arm and forearm was a 180° elbow extension (arm fully extended), the angle between the upper body and shoulder was 0° and the wrist is in neutral position (Figure 8). The same 4 forces were tested at 20, 30, 40, and 50 N.

For each configuration, the subject was asked to hold the handle without applying any grip force. After the correct posture and push force were established, the vibration data were measured. The subject was requested to maintain a constant push force during the test using the DC force displayed by the force
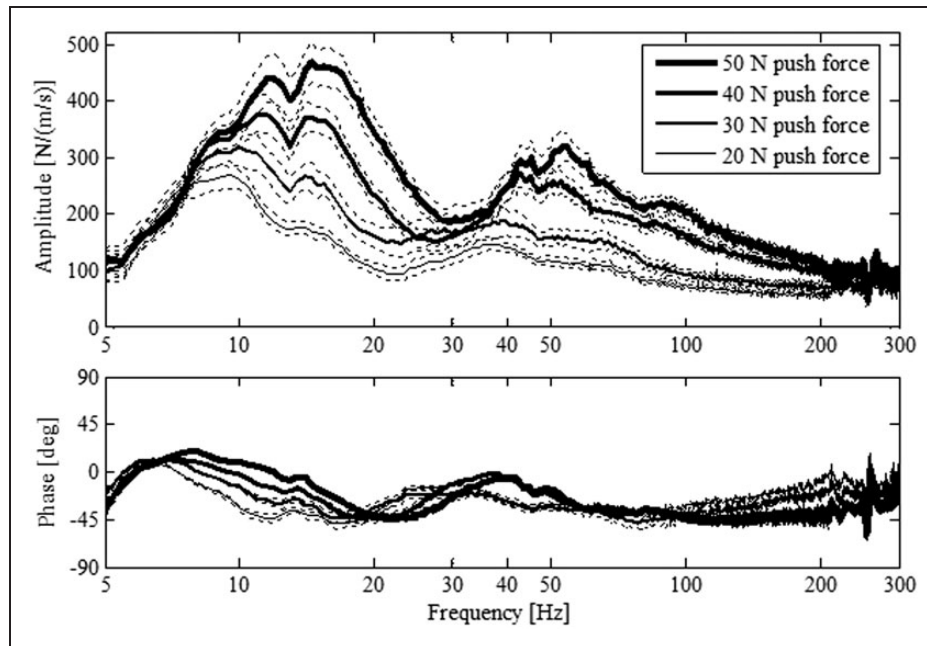

Figure 8. Posture for excitation of the hand along the vertical axis.

sensor. A total of 10 measurements were performed for each configuration to evaluate intra-subject variability. The measurements were carried out over several days to avoid subject fatigue.

3. Results

3.1. Hand-arm system impedance

The results of the hand-arm system impedance measurements for the selected posture and the 4 push forces are illustrated in Figure 9 in terms of amplitude and phase. The measured impedances depict the
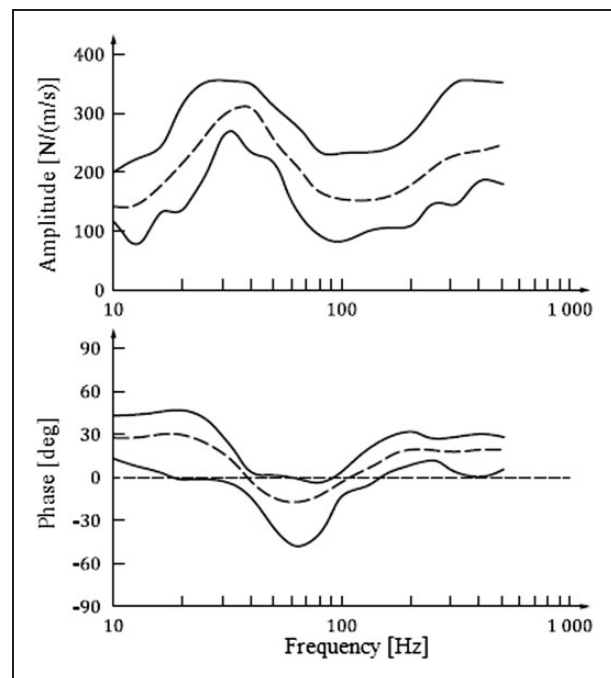
Figure 9. Mechanical impedance of the hand-arm system along the vertical axis.

biodynamic behaviour of the hand-arm system for this specific posture and type of excitation. Each curve in solid line represents the mean of the 10 measured FRFs for each push force. The dotted lines around the mean correspond to the 95 % confidence interval for each push force.

Typically, the hand-arm system impedance amplitude increases with the push force. For each push force, the results indicate two damped peaks in the frequency range of 10–75 Hz. This reveals a more important influence of the dynamic behaviour of the hand-arm system with this specific posture along the vertical axis for frequencies between 10 and 75 Hz.

There are some differences in the hand-arm impedance presented on Figure 9 compared to the ISO-10068 document (2012) on idealized hand-arm impedance. The magnitude peaks occur at much lower frequencies and the phase is also quite different. It is important to remember that the measured impedances in Figure 9 depict the biodynamic behaviour of the hand-arm system for this specific posture and type of excitation. Despite the fact that the ISO-10068 document presents relatively broad ranges of the hand-arm system impedance, some conditions are different from the ones used in this manuscript; (1) the angle between the forearm and upper arm is different, (2) there is no grip force in the manuscript. These differences in conditions between the ISO-10068 document and this manuscript probably explain some of the differences. Other reasons could also be considered for the differences. Despite the differences, the phase range is between $-45°$ and $45°$ in both ISO-10068 and this manuscript, and the range in

Figure 10. Example of mechanical impedance of the hand-arm system from ISO-10068 (2012).

terms of amplitude is also similar in both cases. An example of hand-arm system impedance from ISO-10068 (2012) is given in Figure 10.

Statistical analysis indicates that the data are normally distributed. For each push force, the largest uncertainty level on the impedance curves is observed around

15 Hz. Furthermore, deviation from the mean leading to a 95% confidence interval for each push force can be determined based on the standard deviation. The maximum deviation from the mean leading to a 95% confidence interval is presented in Table 1 for each force.

Results shown in Table 1 indicate that the standard deviation rises with the push force. Furthermore, in Figure 9, below 200 Hz, the curves are well dissociated. Considering the standard deviations, this means that each push force can be distinguished on the hand-arm system impedance responses.

Table 1. Maximum deviation from the mean leading to a 95% confidence interval on the hand-arm system impedance in terms of amplitude for each push force.
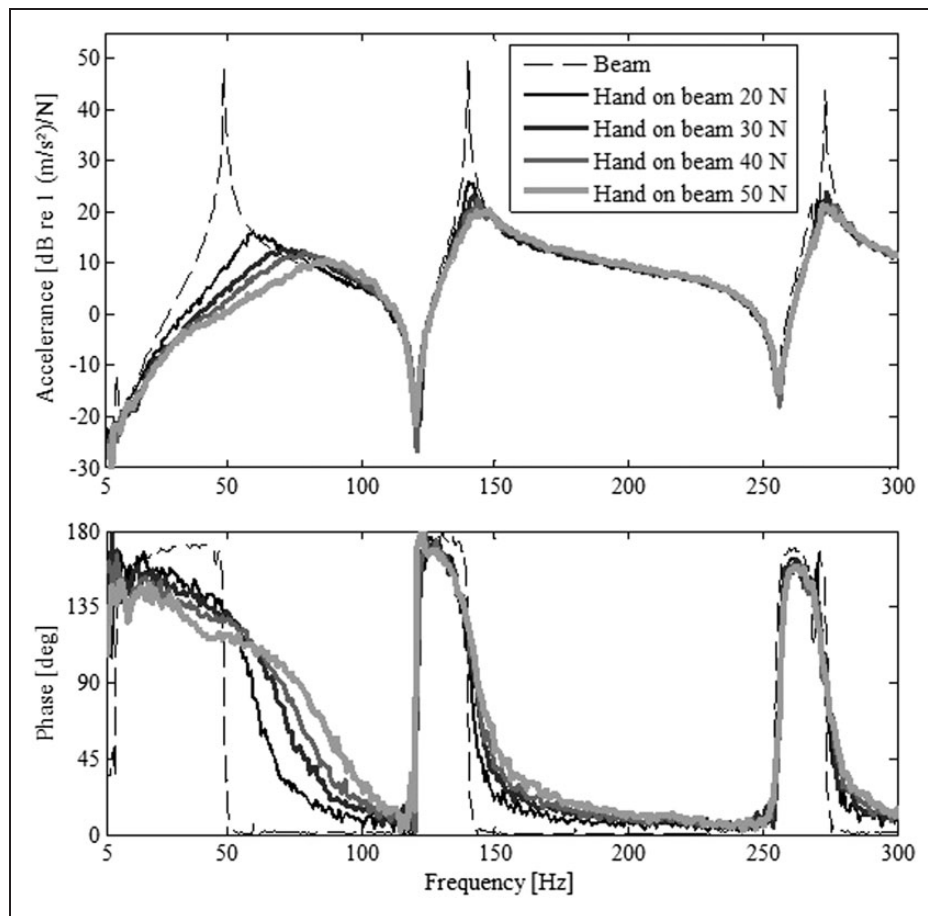
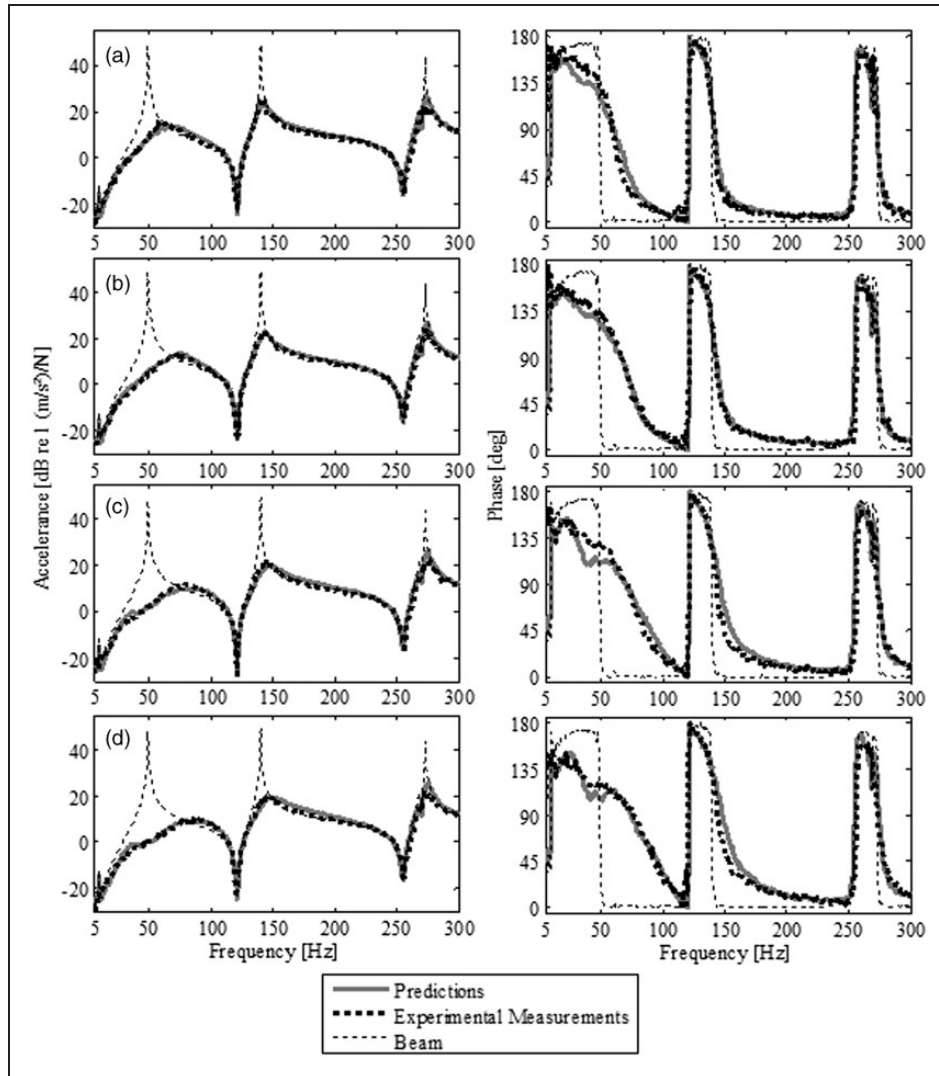| Push force (N)	Maximum deviation (N/(m/s))
20	27.4
30	36.9
40	35.3
50	43.8

3.2. Dynamic behaviour of the coupled system

The beam dimensions were selected to reveal multiple modes in the frequency range of interest 5–300 Hz. The Figure 11 shows the accelerance measured at the hand for the 4 push forces. It illustrates the influence of the hand on the beam in terms of amplitude and phase.

In Figure 11, the measured FRF of the beam without the hand shows three resonances at 49, 140, and 273 Hz in alternation with anti-resonances at 121 and 255 Hz since it is a driving-point FRF. It can clearly be seen that the dynamic behaviour of the beam is modified when the hand-arm system applies a push force. Furthermore, the influence of the hand-arm system on the beam is not the same for the 4 different push forces. This highlights the importance of controlling the push forces. The hand-arm system has an influence on each of the modes but most specifically on the first resonance. For the second and third resonances, the hand-arm system mainly adds damping.

Besides, at low frequencies, the measurements with beam alone show the phase around 40 degrees. This is certainly due to inaccuracies in the measurements. As in

Figure 11. Vibrational behaviour of the beam and measured influence of the hand on the beam's vibrational behaviour for the four push forces.

Figure 12. Coupling predictions of the hand on the beam for the vertical axis and the specific posture compared to the experimental data for the 4 push forces (a: 20 N, b: 30 N, c: 40 N and d: 50 N) in amplitude (left) and phase (right).

case of the ISO-10068 standard, results may be considered above 10 Hz.

3.3. Comparison between coupling models and experimental measurements

In this section, the experimental FRF of the beam is coupled with the experimental FRFs of the hand-arm system's dynamic characteristics using the substructuring approach. The predicted values for the dynamic behaviour of the coupled system using this approach (equation (11)) with a specific posture and 4 different push forces are compared to the experimental measurements performed on the coupled system with the same posture and push forces. The dynamic behaviour of the beam alone is indicated in the dotted line to highlight the influence of the hand on the beam. The maximum

standard deviation for each predicted value is less than 1.5 dB in terms of acceleration $[(m/s^2)/N]$.

4. Discussion

This work illustrates the reliability of the substructuring approach by using one specific position, one direction of excitation, and by controlling the push forces applied. Since the mechanical behaviour of the human body is sensitive to several factors such as position and posture, excitation direction, forces, and others, these factors should be controlled. The beam was used only to demonstrate the reliability of predictions that can be obtained using this approach. For future research, any other compliant mechanical structure normally in contact with the human body could be tested using substructuring techniques to predict their dynamic

behaviour changes. Furthermore, according to the equations, coupling with a mechanical structure can involve more than just one interface point. Mechanical couplings can also involve more than one direction by taking into account more DOFs in the coupling process. This can allow, for example, investigating multi-axis effects as well as 3D vibrations in the three orthogonal directions on the human body.

The characterization of the human body could be either an experimental measurement, to account for intra- and inter-subject variability, or an analytical model, for general analysis, as long as the FRFs are available. In fact, it does not make any significant difference to directly use the measured impedance for the coupling or to use a hand-arm model to predict the dynamic behaviour of the assembly, as long as the model provides a reasonable simulation of the measured response functions. Likewise, the dynamic characterization of the mechanical structure could be provided either through experimentation or FE model. Using the FE results during the development phase of a structure, the substructuring techniques approach can conceivably be used to improve the dynamic behaviour of the mechanical structure prior to production while taking into account the influence of the biodynamic characteristics.

According to this study on coupling human hand-arm system biodynamic characterizations with a mechanical structure, substructuring techniques appear to have great potential to predict human influence on compliant mechanical structures in the context of vibration exposure. Its potential can be extended in order to use this approach for any part of the human body or even for the entire body, such as whole-body vibration or vibrations experienced when in a seated position. For example, research into the biodynamic modeling of seated occupants exposed to whole-body vibration has resulted in the development of effective models and construction of anthropodynamic manikins to analyze and test automotive and suspension seats (Boileau et al., 1997; Lewis, 2000). Whole body-seat interactions are the focus of the International Standard ISO-5982 (ISO-5982) (2001); this standard establishes the range of idealized values to characterize seated-body biodynamic responses under vertical vibration in order to evaluate the coupling effects with seats. In the field of automotive engineering and transportation, the use of a substructuring technique would prove useful in predicting the influence of seated occupants on the dynamic behaviour of seats or suspension systems. This approach may also prove to be useful in studying lightweight and highly compliant sports equipment.

Among the several advantages of the substructuring approach, this work highlighted the following:

1. Direct use of shaker test data;
2. Utilization of both analytic and experimental results;
3. Combination of substructures when only the data interfaces are known;
4. Reduction of model size so that only relevant degrees of freedom need to be considered;
5. Hybrid use of experimental and FE FRFs.

It is believed these five main approach advantages will be beneficial in further predicting human influence on compliant structures in order to anticipate the reduction of transmitted vibration.

5. Conclusion

The aim of this study was to provide an approach to predicting human influence on compliant mechanical structures using a substructuring technique. Equations corresponding to this approach were formulated. More specifically in this study, a demonstration was conducted using the hand-arm system. The results shown in Figure 12 demonstrate that the substructuring approach can provide reliable predictions. The influence of the human hand on the beam depends on the push force (Figure 11). It is thus important to control the push force applied by the subject because the response of the hand-arm system in terms of impedance is sensitive to this parameter (Figure 9). By dint of this consideration, the model can predict the hand-arm system's influence on a beam's dynamic behaviour with 4 different push forces.

This study highlighted the feasibility of predicting the influence of the hand-arm system on a compliant mechanical structure by using the substructuring approach with biodynamics and by controlling the posture and the contact forces. The results of this study indicate that this is a promising approach to coupling compliant mechanical structures with the human body and predicting the dynamic behavior of the assembly, in the context of vibration exposure.

Conflict of interest
The authors report no conflict of interest.

Funding

References
Adewusi SA, Rakheja S, Marcotte P and Boileau PE (2008) On the discrepancies in the reported human hand-arm impedance at higher frequencies. *International Journal of Industrial Ergonomics* 38: 703–714.

Aldien Y, Marcotte P, Rakheja S and Boileau PE (2005) Mechanical impedance and absorbed power of hand-arm

under xh-axis vibration and role of hand forces and posture. *Industrial Health* 43: 495–508.

Aldien Y, Marcotte P, Rakheja S and Boileau PE (2006) Influence of hand-arm posture on biodynamic response of the human hand-arm exposed to z_h-axis vibration. *International Journal of Industrial Ergonomics* 36: 45–59.

Avitabile P (2003) Twenty Years of Structural Dynamic Modification: A Review. *Sound and Vibration* 37: 14–25.

Besa AJ, Valero FJ, Suñer JL and Carballeira J (2007) Characterization of the mechanical impedance of the human hand arm system: The influence of vibration direction, hand arm posture and muscle tension. *International Journal of Industrial Ergonomics* 37: 225–231.

Boileau PE, Rakheja S, Yang X and Stiharu I (1997) Comparison of biodynamic response characteristics of various human body models as applied to seated vehicle drivers. *Noise and Vibration Worldwide* 28: 7–15.

Burström L (1990) *Absorption of Vibration Energy in the Human Hand-Arm*. PhD Thesis, Lulea University of Technology.

Burström L (1997) The influence of biodynamic factors on the mechanical impedance of the hand and arm. *International Archives of Occupational and Environmental Health* 69: 437–446.

Craig R and Bampton M (1968) Coupling of Substructures for Dynamic Analysis. *AIAA Journal* 6: 1313–1319.

Daikoku M and Ishikawa F (1990) Mechanical impedance and vibration model of hand – arm system, *Proceedings of the Fifth International conference on Hand-Arm Vibration*, Kanzawa, Japan.

De Klerk D, Rixen DJ and Voormeeren SN (2008) General Framework for Dynamic Substructuring: History, Review, and Classification of Techniques. *AIAA Journal* 46: 1169–1181.

Dong RG, Rakheja S, Schopper AW, Han B and Smutz WP (2001) Hand-transmitted vibration and biodynamic response of the human hand–arm: a critical review. *Critical Reviews in Biomedical Engineering* 29: 391–441.

Dong RG, Welcome DE, McDowell TW and Wu JZ (2006) Measurement of biodynamic response of human hand-arm system. *Journal of Sound and Vibration* 294: 807–827.

Dong RG, Welcome DE, McDowell TW and Wu JZ (2008a) Analysis of handle dynamics-induced errors in hand biodynamic measurements. *Journal of Sound and Vibration* 318: 1313–1333.

Dong RG, Welcome DE, Wu JZ and McDowell TW (2008b) Development of hand-arm system models for vibrating tool analysis and test rig construction. *Noise Control Engineering Journal* 56: 35–44.

Dong RG, Welcome DE, Xu XS, Warren C, McDowell TW, Wu JZ, et al. (2012) Mechanical impedances distributed at the fingers and palm of the human hand in three orthogonal directions. *Journal of Sound and Vibration* 331: 1191–1206.

Dong RG, Wu JZ and Welcome DE (2005) Recent advances in biodynamics of hand-arm system. *Industrial Health* 43: 449–471.

Ewins DJ (2000) *Modal Testing: theory, practice and application*, 2nd edition. Philadelphia: Research Studies Press.

Griffin MJ (1990) *Handbook of Human Vibration*. London: Academic Press.

Griffin MJ (1994) Foundations of hand-transmitted vibration standards. *Nagoya Journal of Medical Science* 57(Suppl.): 147–164.

Gurram R, Rakheja S and Brammer AJ (1995) Driving-point mechanical impedance of the human hand-arm system: synthesis and model development. *Journal of Sound and Vibration* 180: 437–458.

Hurty WC (1960) Vibrations of Structural Systems by Component Mode Synthesis. *Journal of Engineering Mechanics/American Society of Civil Engineers* 86: 51–69.

Imregun M and Robb D (1992), Structural Modification via FRF Coupling Using Measured Data. *Proceedings of the Tenth International Modal Analysis Conference*, Society for Experimental Mechanics, pp. 1095–1099.

International Organization for Standardization 5982 (ISO-5982) (2001) Mechanical vibration and shock – Range of idealized values to characterize seated-body biodynamic response under vertical vibration. *International Standard* ISO-5982.

International Organization for Standardization 5349 (ISO-5349) (2001) Mechanical vibration – Measurement and evaluation of human exposure to hand-transmitted vibration. *International Standard* ISO-5349.

International Organization for Standardization 10068 (ISO-10068) (2012) Mechanical vibration and shock, mechanical impedance of the human hand – arm system at the driving point, *International Standard* ISO-10068.

Jahn R and Hesse M (1986) Applications of hand-arm models in the investigation of the interaction between man and machine. *Scandinavian Journal of Work, Environment and Health* 12: 343–346.

Jetmundsen B (1986) *On frequency domain methodologies for prescribed structural modification and subsystem synthesis*. PhD Thesis, Rensselaer Polytechnic Institute, New York.

Jetmundsen B, Bielawa R and Flanelly W (1988) Generalized Frequency Domain Substructure Synthesis. *Journal of the American Helicopter Society* 33: 55–65.

Lewis CH (2000) Evaluating the vibration isolation of soft seats using an active anthropodynamic dummy. *Proceedings of 35th UK Group Meeting on Human Responses to Vibration*, Southampton, England, pp. 249–259.

MacNeal R (1971) Hybrid Method of Component Mode Synthesis. *Computers and Structures* 1(4): 581–601.

Mansfield NJ (2005) *Human Response to Vibration*. Boca Raton: CRC Press.

Marcotte P, Adewusi S, Boutin J, Nélisse H, Rakheja S and Boileau PE (2007) Modeling the contributions of handle dynamics on the biodynamic response of the human hand-arm system. *11th International Conference on Hand-Arm Vibration*, Bologna.

Marcotte P, Aldien Y, Boileau PE, Rakheja S and Boutin J (2005) Effect of handle size and hand-handle contact force on the biodynamic response of the hand-arm system under z_h–axis vibration. *Journal of Sound and Vibration* 283: 1071–1091.

Marcotte P, Boutin J and Jasinski J (2010) Development of a hand-arm mechanical analogue for evaluating chipping hammer vibration emission values. *Journal of Sound and Vibration* 329: 1068–1980.

Mishoe JW and Suggs CW (1977) Hand-arm vibration. Part II. Vibrational responses of the human hand. *Journal of Sound and Vibration* 53: 545–558.

Rakheja S, Wu JZ, Dong RG and Schopper AW (2002) A comparison of biodynamic models of the human hand-arm system for applications to hand-held power tools. *Journal of Sound and Vibration* 249: 55–82.

Reynolds DD and Falkenberg RJ (1982) Three- and four-degrees of freedom models of the vibration response of the human hand. In: Brammer AJ and Taylor W (eds) *Vibration Effects on the Hand and Arm in Industry* pp. 117–132.

Reynolds DD and Falkenberg RJ (1984) A study of hand vibration on chipping and grinding operators. Part II: four-degree-of-freedom lumped parameter model of the vibration response of the human hand. *Journal of Sound and Vibration* 95: 499–514.

Reynolds DD and Soedel W (1977) Dynamic response of the hand – arm system to a sinusoidal input. *Journal of Sound and Vibration* 21: 339–353.

Rubin S (1975) Improved Component-Mode Representation for Structural Dynamic Analysis. *AIAA Journal* 13: 995–1006.

Appendix 1: frequency – based Substructuring formulation

The purpose of this appendix is to formulate the substructuring approach in terms of Mobility or Admittance formulation. While the impedance formulation allows us to characterize a structure with an excitation in terms of velocity and a response in terms of blocked force, the admittance formulation allows us to characterize a structure in free-free conditions with an excitation in terms of force and a response in terms of velocity.
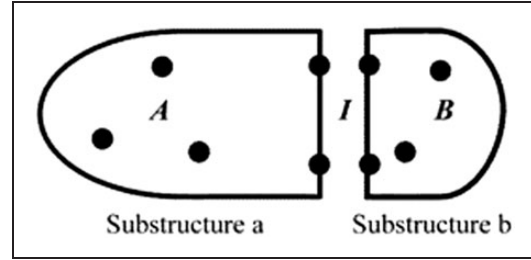
Consider two structures "a" and "b" that are coupled to form an assembly "ab" (Figure 13). Set A represents the set of internal degrees of freedom (DOFs) for substructure "a" while set B represents the set of internal DOFs for substructure "b". Set I represents the set of interface DOFs for substructure "a" and substructure "b".

These two substructures can be described by a mobility or admittance formulation. Admittance is the inverse of Impedance. If we consider the dynamics of each substructure separately, we can write the following equation for substructure "a":

$$\left\{ \begin{array}{c} \mathbf{V}_A^a(\omega) \\ \mathbf{V}_I^a(\omega) \end{array} \right\} = \left[\begin{array}{cc} \mathbf{Y}_{AA}^a(\omega) & \mathbf{Y}_{AI}^a(\omega) \\ \mathbf{Y}_{IA}^a(\omega) & \mathbf{Y}_{II}^a(\omega) \end{array} \right] \left\{ \begin{array}{c} \mathbf{F}_A^a(\omega) \\ \mathbf{F}_I^a(\omega) \end{array} \right\} \qquad (13)$$

And similarly for substructure "b"

$$\left\{ \begin{array}{c} \mathbf{V}_I^b(\omega) \\ \mathbf{V}_B^b(\omega) \end{array} \right\} = \left[\begin{array}{cc} \mathbf{Y}_{II}^b(\omega) & \mathbf{Y}_{IB}^b(\omega) \\ \mathbf{Y}_{BI}^b(\omega) & \mathbf{Y}_{BB}^b(\omega) \end{array} \right] \left\{ \begin{array}{c} \mathbf{F}_I^b(\omega) \\ \mathbf{F}_B^b(\omega) \end{array} \right\} \qquad (14)$$

Figure 13. Example of a coupling between two substructures "a" and "b" where substructure "a" has five points of interest (two of them are in the interface set *I* and three are in the internal set *A*) and substructure "b" has four points of interest (two of them are in the interface set *I* to match those of substructure "a" and two are in the internal set *B*).

In the same way, we can write the admittance version of the FRF matrix for the system "ab"

$$\left\{ \begin{array}{c} \mathbf{V}_A^{ab}(\omega) \\ \mathbf{V}_I^{ab}(\omega) \\ \mathbf{V}_B^{ab}(\omega) \end{array} \right\} = \left[\begin{array}{ccc} \mathbf{Y}_{AA}^{ab}(\omega) & \mathbf{Y}_{AI}^{ab}(\omega) & \mathbf{Y}_{AB}^{ab}(\omega) \\ \mathbf{Y}_{IA}^{ab}(\omega) & \mathbf{Y}_{II}^{ab}(\omega) & \mathbf{Y}_{IB}^{ab}(\omega) \\ \mathbf{Y}_{BA}^{ab}(\omega) & \mathbf{Y}_{BI}^{ab}(\omega) & \mathbf{Y}_{BB}^{ab}(\omega) \end{array} \right] \left\{ \begin{array}{c} \mathbf{F}_A^{ab}(\omega) \\ \mathbf{F}_I^{ab}(\omega) \\ \mathbf{F}_B^{ab}(\omega) \end{array} \right\} \qquad (15)$$

For sake of simplicity in the following equations, the frequency-dependency (ω) of the various terms is not written. By an application of the equilibrium and compatibility conditions at the interface set of DOFs, one can derive an admittance version of the FRF matrix for the coupled structure "ab" based on the admittance characterization of each substructure separately

$$\left[\begin{array}{ccc} \mathbf{Y}_{AA} & \mathbf{Y}_{AI} & \mathbf{Y}_{AB} \\ \mathbf{Y}_{IA} & \mathbf{Y}_{II} & \mathbf{Y}_{IB} \\ \mathbf{Y}_{BA} & \mathbf{Y}_{BI} & \mathbf{Y}_{BB} \end{array} \right]^{ab} = \left[\begin{array}{ccc} \mathbf{Y}_{AA}^a & \mathbf{Y}_{AI}^a & 0 \\ \mathbf{Y}_{IA}^a & \mathbf{Y}_{II}^a & 0 \\ 0 & 0 & \mathbf{Y}_{BB}^b \end{array} \right] - \left\{ \begin{array}{c} \mathbf{Y}_{AI}^a \\ \mathbf{Y}_{II}^a \\ -\mathbf{Y}_{BI}^b \end{array} \right\}$$
$$\times \left[\mathbf{Y}_{II}^a + \mathbf{Y}_{II}^b \right]^{-1} \left\{ \begin{array}{c} \mathbf{Y}_{AI}^a \\ \mathbf{Y}_{II}^a \\ -\mathbf{Y}_{BI}^b \end{array} \right\}^{T} \qquad (16)$$

As an approach to studying human-structure interactions where a human being is coupled to a vibrating structure, the substructuring techniques offer some advantages that can be used either with biodynamic measurements, representative models, or other characterizations of the human body. One of these advantages is the opportunity of coupling substructures through a consideration of their interface set only. Literally speaking, substructure "a" being the mechanical structure, substructure "b" being the human body, and interface I being the contact between the human body and the mechanical structure, set B represents the set of internal DOFs that could be anywhere on the human

body. Since only interface measurements can be gathered for the human body, namely the driving-point, equation (16) can be simplified to leave out the set of internal DOFs B

$$
\begin{bmatrix} \mathbf{Y}_{AA} & \mathbf{Y}_{AI} \\ \mathbf{Y}_{IA} & \mathbf{Y}_{II} \end{bmatrix}^{ab} = \begin{bmatrix} \mathbf{Y}_{AA}^{a} & \mathbf{Y}_{AI}^{a} \\ \mathbf{Y}_{IA}^{a} & \mathbf{Y}_{II}^{a} \end{bmatrix}
$$
$$
- \left\{ \begin{matrix} \mathbf{Y}_{AI}^{a} \\ \mathbf{Y}_{II}^{a} \end{matrix} \right\} [\mathbf{Y}_{II}^{a} + \mathbf{Y}_{II}^{b}]^{-1} \left\{ \begin{matrix} \mathbf{Y}_{AI}^{a} \\ \mathbf{Y}_{II}^{a} \end{matrix} \right\}^{T}
$$
$$
\tag{17}
$$

Equation (17) is the generalized equation of the substructuring approach with biodynamics in terms of FBS formulation. There can be as many DOFs as necessary for the internal set A and the interface set I.